

 $^{13,14}\text{B}(n, \gamma)$  via Coulomb Dissociation for Nucleosynthesis towards the  $r$ -Process

S.G. Altstadt,<sup>1,2,\*</sup> T. Adachi,<sup>3</sup> Y. Aksyutina,<sup>2,4</sup> J. Alcantara,<sup>5</sup> H. Alvarez-Pol,<sup>5</sup> N. Ashwood,<sup>6</sup> L. Atar,<sup>7</sup> T. Aumann,<sup>7,2</sup> V. Avdeichikov,<sup>8</sup> M. Barr,<sup>6</sup> S. Beceiro,<sup>5</sup> D. Bemmerer,<sup>9</sup> J. Benlliure,<sup>5</sup> C.A. Bertulani,<sup>10</sup> K. Boretzky,<sup>2</sup> M.J.G. Borge,<sup>11</sup> G. Burgunder,<sup>12</sup> M. Caamano,<sup>5</sup> C. Caesar,<sup>7</sup> E. Casarejos,<sup>13</sup> W. Catford,<sup>14</sup> J. Cederkäll,<sup>8</sup> S. Chakraborty,<sup>15</sup> M. Chartier,<sup>16</sup> L. Chulkov,<sup>17,4</sup> D. Cortina-Gil,<sup>5</sup> U. Datta Pramanik,<sup>15</sup> P. Diaz Fernandez,<sup>5</sup> I. Dillmann,<sup>2</sup> Z. Elekes,<sup>9</sup> J. Enders,<sup>7</sup> O. Ershova,<sup>1</sup> A. Estrade,<sup>2</sup> F. Farinon,<sup>2</sup> L.M. Fraile,<sup>18</sup> M. Freer,<sup>6</sup> M. Freudenberger,<sup>7</sup> H.O.U. Fynbo,<sup>19</sup> D. Galaviz,<sup>20</sup> H. Geissel,<sup>2</sup> R. Gernhäuser,<sup>21</sup> K. Göbel,<sup>1</sup> P. Golubev,<sup>8</sup> D. Gonzalez Diaz,<sup>7</sup> J. Hagdahl,<sup>22</sup> T. Heftrich,<sup>1</sup> M. Heil,<sup>2</sup> M. Heine,<sup>7</sup> A. Heinz,<sup>22</sup> A. Henriques,<sup>20</sup> M. Holl,<sup>7</sup> J.D. Holt,<sup>23,24</sup> G. Ickert,<sup>2</sup> A. Ignatov,<sup>7</sup> B. Jakobsson,<sup>8</sup> H.T. Johansson,<sup>22</sup> B. Jonson,<sup>22</sup> N. Kalantar-Nayestanaki,<sup>3</sup> R. Kanungo,<sup>25</sup> A. Kelic-Heil,<sup>2</sup> R. Knöbel,<sup>2</sup> T. Kröll,<sup>7</sup> R. Krücken,<sup>21</sup> J. Kurcewicz,<sup>2</sup> N. Kurz,<sup>2</sup> M. Labiche,<sup>26</sup> C. Langer,<sup>1</sup> T. Le Bleis,<sup>21</sup> R. Lemmon,<sup>26</sup> O. Lepyoshkina,<sup>21</sup> J. Machado,<sup>20</sup> J. Marganec,<sup>4</sup> V. Maroussov,<sup>27</sup> J. Menéndez,<sup>7,4</sup> M. Mostazo,<sup>5</sup> A. Movsesyan,<sup>7</sup> M.A. Najafi,<sup>3</sup> T. Nilsson,<sup>22</sup> C. Nociforo,<sup>2</sup> V. Panin,<sup>7</sup> A. Perea,<sup>11</sup> S. Pietri,<sup>2</sup> R. Plag,<sup>1</sup> A. Prochazka,<sup>2</sup> A. Rahaman,<sup>15</sup> G. Rastrepina,<sup>2</sup> R. Reifarth,<sup>1</sup> G. Ribeiro,<sup>11</sup> M.V. Ricciardi,<sup>2</sup> C. Rigollet,<sup>3</sup> K. Riisager,<sup>19</sup> M. Röder,<sup>28,9</sup> D. Rossi,<sup>2</sup> J. Sanchez del Rio,<sup>11</sup> D. Savran,<sup>4,29</sup> H. Scheit,<sup>7</sup> A. Schwenk,<sup>4,7</sup> H. Simon,<sup>2</sup> J. Simonis,<sup>7,4</sup> K. Sonnabend,<sup>1</sup> O. Sorlin,<sup>12</sup> V. Stoica,<sup>3</sup> B. Streicher,<sup>3</sup> J. Taylor,<sup>16</sup> O. Tengblad,<sup>11</sup> S. Terashima,<sup>2</sup> R. Thies,<sup>22</sup> Y. Togano,<sup>4</sup> E. Uberseder,<sup>30</sup> J. Van de Walle,<sup>3</sup> P. Velho,<sup>20</sup> V. Volkov,<sup>7</sup> A. Wagner,<sup>9</sup> F. Wamers,<sup>7,2</sup> H. Weick,<sup>2</sup> M. Weigand,<sup>1</sup> C. Wheldon,<sup>6</sup> G. Wilson,<sup>31</sup> C. Wimmer,<sup>1</sup> J.S. Winfield,<sup>2</sup> P. Woods,<sup>32</sup> D. Yakorev,<sup>9</sup> M.V. Zhukov,<sup>22</sup> A. Zilges,<sup>27</sup> M. Zoric,<sup>2</sup> and K. Zuber<sup>28</sup>

(R<sup>3</sup>B collaboration)<sup>1</sup>Goethe-Universität Frankfurt am Main, D-60438 Frankfurt am Main, Germany<sup>2</sup>GSI Helmholtzzentrum für Schwerionenforschung, D-64291 Darmstadt, Germany<sup>3</sup>KVI, University of Groningen, Zernikelaan 25, NL-9747 AA Groningen, The Netherlands<sup>4</sup>ExtreMe Matter Institute EMMI, GSI Helmholtzzentrum für Schwerionenforschung GmbH, 64291 Darmstadt, Germany<sup>5</sup>Departamento de Física de Partículas, Universidade de Santiago de Compostela, 15706 Santiago de Compostela, Spain<sup>6</sup>School of Physics and Astronomy, University of Birmingham, Birmingham B15 2TT, United Kingdom<sup>7</sup>Institut für Kernphysik, Technische Universität Darmstadt, D-64289 Darmstadt, Germany<sup>8</sup>Department of Physics, Lund University, S-22100 Lund, Sweden<sup>9</sup>Helmholtz-Zentrum Dresden-Rossendorf, D-01328 Dresden, Germany<sup>10</sup>Department of Physics and Astronomy, Texas A&M University-Commerce, Commerce, Texas 75429, USA<sup>11</sup>Instituto de Estructura de la Materia, CSIC, Serrano 113 bis, E-28006 Madrid, Spain<sup>12</sup>Grand Accélérateur National d'Ions Lourds (GANIL),

CEA/DSM-CNRS/IN2P3, B.P. 55027, F-14076 Caen Cedex 5, France

<sup>13</sup>University of Vigo, E-36310 Spain<sup>14</sup>Department of Physics, University of Surrey, Guildford GU2 5FH, United Kingdom<sup>15</sup>Saha Institute of Nuclear Physics, 1/AF Bidhan Nagar, Kolkata-700064, India<sup>16</sup>Oliver Lodge Laboratory, University of Liverpool, Liverpool L69 7ZE, United Kingdom<sup>17</sup>Kurchatov Institute, Ru-123182 Moscow, Russia<sup>18</sup>Facultad de Ciencias Físicas, Universidad Complutense de Madrid, Avda. Complutense, E-28040 Madrid, Spain<sup>19</sup>Department of Physics and Astronomy, Aarhus University, DK-8000 Århus C, Denmark<sup>20</sup>Centro de Física Nuclear, University of Lisbon, P-1649-003 Lisbon, Portugal<sup>21</sup>Physik Department E12, Technische Universität München, 85748 Garching, Germany<sup>22</sup>Fundamental Fysik, Chalmers Tekniska Högskola, S-412 96 Göteborg, Sweden<sup>23</sup>Department of Physics and Astronomy, University of Tennessee, Knoxville, TN 37996, USA<sup>24</sup>Physics Division, Oak Ridge National Laboratory, P.O. Box 2008, Oak Ridge, TN 37831, USA<sup>25</sup>Astronomy and Physics Department, Saint Mary's University, Halifax, NS B3H 3C3, Canada<sup>26</sup>STFC Daresbury Laboratory, Daresbury, Warrington WA4 4AD, United Kingdom<sup>27</sup>Institut für Kernphysik, Universität zu Köln, D-50937 Köln, Germany<sup>28</sup>Institut für Kern- und Teilchenphysik, Technische Universität, D-01069 Dresden, Germany<sup>29</sup>Frankfurt Institut for Advanced Studies FIAS, Frankfurt, Germany<sup>30</sup>Department of Physics, University of Notre Dame, Notre Dame, Indiana 46556, USA<sup>31</sup>Department of Physics, University of Surrey, Guildford GU2 5XH, United Kingdom

<sup>32</sup>*School of Physics and Astronomy, University of Edinburgh, Edinburgh EH9 3JZ, United Kingdom*

Radioactive beams of  $^{14,15}\text{B}$  produced by fragmentation of a primary  $^{40}\text{Ar}$  beam were directed onto a Pb target to investigate the neutron breakup within the Coulomb field. The experiment was performed at the LAND/R<sup>3</sup>B setup. Preliminary results for the Coulomb dissociation cross sections as well as for the astrophysically interesting inverse reactions,  $^{13,14}\text{B}(n,\gamma)$ , are presented.

## I. INTRODUCTION

It is known that the rapid neutron capture process ( $r$  process) produces about half of the elements heavier than iron. However, the nuclear physics properties of the involved nuclei are not well known and its astrophysical site is not yet identified. The neutrino-driven wind model within core-collapse supernovae is currently one of the most promising candidate for a successful  $r$  process [1, 2]. Neutrino winds are thought to dissociate all previously formed elements into protons, neutrons and  $\alpha$  particles before the seed nuclei for the  $r$  process are produced. Hence, the neutrino-driven wind model could explain the observational fact that the abundances of  $r$  nuclei in old halo-stars are similar to our solar  $r$ -process abundances [3]. This also indicates that the  $r$  process is a primary process and, thus, independent of the chemical composition of the progenitor star. Therefore, the investigation of the nuclear reactions among light elements forming seed nuclei prior to the  $r$  process leads to a better understanding of this process.

Model calculations within a neutrino-driven wind scenario give a crucial change in the final  $r$ -process abundances by extending the nuclear reaction network towards very light neutron-rich nuclei [4]. Subsequent sensitivity studies point out the most important reactions, which include successive  $(n,\gamma)$  reactions running through the isotopic chain of the neutron-rich boron isotopes  $^{11}\text{B}(n,\gamma)^{12}\text{B}(n,\gamma)^{13}\text{B}(n,\gamma)^{14}\text{B}(n,\gamma)^{15}\text{B}(e^-, \nu)$  followed by a  $\beta$ -decay of  $^{15}\text{B}$  to  $^{15}\text{C}$  [5]. Almost all reaction rates used in these model calculations are only known theoretically. Since the reaction rates of unstable isotopes are very difficult to determine experimentally, neutron breakup reactions of the isotopes  $^{14}\text{B}$  and  $^{15}\text{B}$ , were investigated in inverse kinematics via Coulomb dissociation.

## II. EXPERIMENTAL TECHNIQUES AND SETUP

The experiment was performed at the LAND/R<sup>3</sup>B-setup (Fig. 1) at the GSI, Darmstadt, Germany. To produce the radioactive beams of  $^{14,15}\text{B}$ , a primary beam of  $^{40}\text{Ar}$  was fragmented on a Be-target at about 500 A MeV and the secondary beam was then directed into the

setup through the GSI fragment separator (FRS). The secondary beam consists of different species of isotopes. Thus, each incoming particle has to be identified by determining the charge of the particle,  $Z$ , and the mass-over-charge-ratio  $A/Z$ . The charge is determined by measuring the energy loss in a position sensitive pin diode (PSP), while  $A/Z$  results from a time-of-flight-measurement between two scintillator detectors. The incoming beam identification is shown in Fig. 2.

After this set of detectors, the beam enters the target area, which is surrounded by a  $4\pi$ - $\gamma$ -detector consisting of 159 NaI crystals. A thick lead target of 2 g/cm<sup>2</sup> was used to measure the electromagnetic breakup. In addition, measurements without a target for background determination and with a carbon target to quantify the breakup reactions caused by nuclear interactions with the target were performed.

The invariant mass method is used to obtain an energy-dependent cross section by reconstructing the excitation energy. Therefore, a measurement in complete kinematics had to be performed by detecting all reaction products on an event-by-event basis. The Large Area Neutron Detector (LAND) was used to measure the neutron time-of-flight and position in an active area of about 2x2 m<sup>2</sup>. The outgoing fragments were detected with a time-of-flight wall (TFW) in order to measure their velocity and energy-loss. A large acceptance dipole magnet (ALADiN) bent the charged fragments according to their mass on their way towards the TFW separating them from the neutrons. Two silicon strip detectors behind the target area and two fiber detectors (consisting of an array of vertically aligned scintillating fibers which are read out by position-sensitive PMTs) [6] after the dipole magnet measured the positions of the outgoing fragments. The information is used to determine the mass of the fragments (if the charge is already known) based on their curved trajectory through the magnetic field. The different masses of the boron isotopes are well separated as illustrated in Fig. 3.

## III. PRELIMINARY RESULTS

The principle of detailed balance is applied to obtain a neutron capture cross-section from the time-reversed reaction measured via Coulomb dissociation. The population of excited states in the exit channel is important, since the detailed balance theorem is only valid for transitions between the same states. The de-excitation occurs

\* Corresponding author: s.altstadt@gsi.de

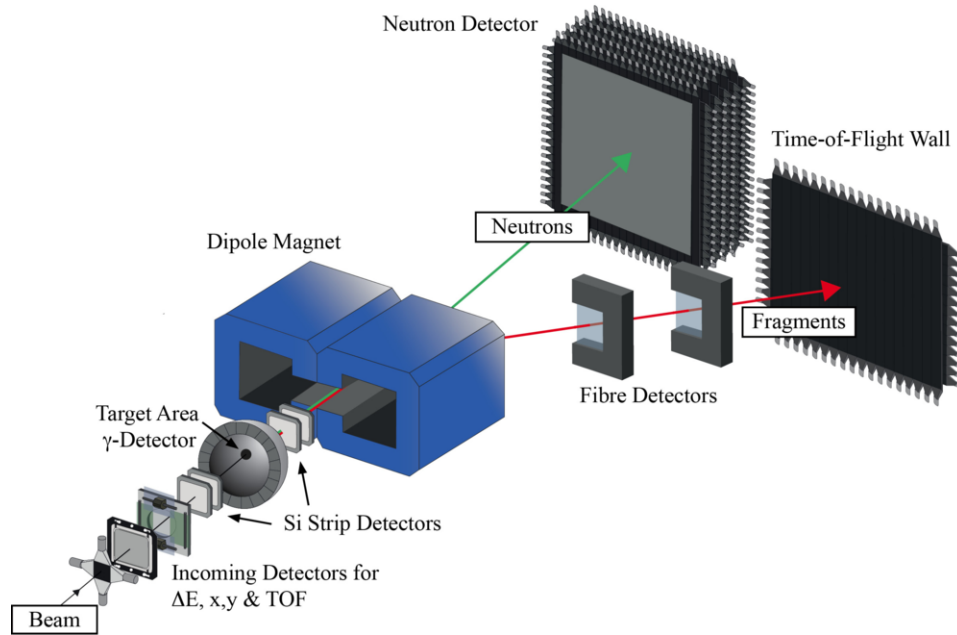


FIG. 1. The LAND/R<sup>3</sup>B setup at the GSI, Darmstadt, Germany.

via  $\gamma$ -emission, which can be detected with the surrounding  $\gamma$ -detector. The population of excited states of each investigated isotope was identified using the Doppler-corrected  $\gamma$ -sum spectra and were excluded on an event-by-event basis.

The differential Coulomb dissociation cross-sections

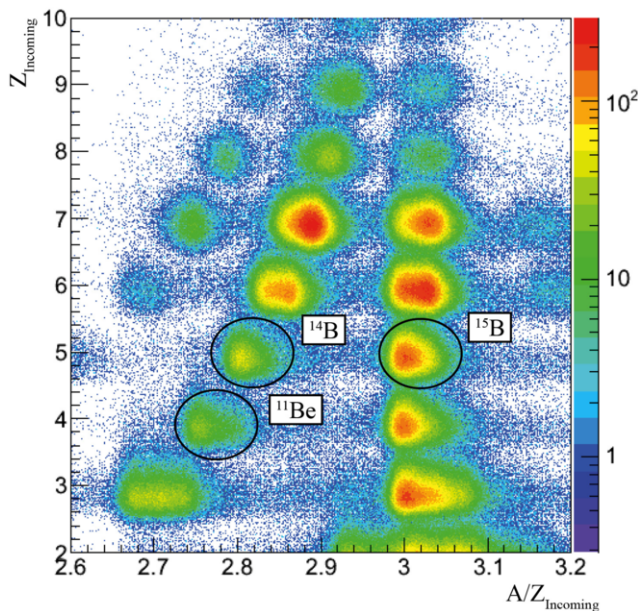


FIG. 2. Identification of incoming particles. The isotopes of interest  $^{14,15}\text{B}$  as well as  $^{11}\text{Be}$ , which was used as a test-case, were produced in the same beam setting.

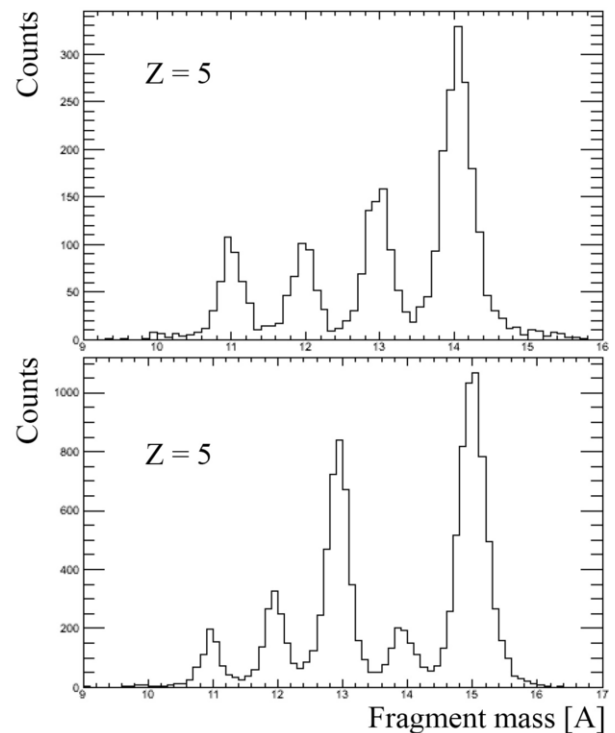


FIG. 3. Tracked masses for  $^{14}\text{B}$  (upper panel) and  $^{15}\text{B}$  (lower panel) to separate the different boron isotopes. The different mass peaks are clearly separated and the influence of nearby masses is very small.

( $d\sigma_{CD}/dE$ ) of  $^{14}\text{B} \rightarrow ^{13}\text{B}+n$  and  $^{15}\text{B} \rightarrow ^{14}\text{B}+n$  are shown in Fig. 4. The preliminary integral cross-sections up to

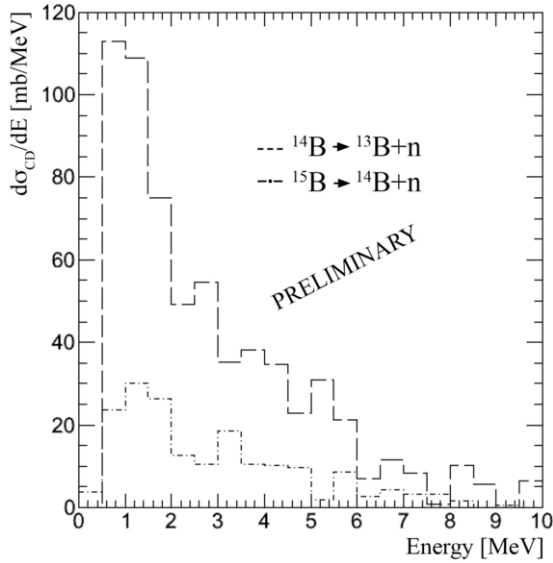


FIG. 4. Differential Coulomb dissociation cross sections for  $^{14}\text{B} \rightarrow ^{13}\text{B}+n$  (dashed line) and  $^{15}\text{B} \rightarrow ^{14}\text{B}+n$  (dotted and dashed line). Contributions from excited states were excluded.

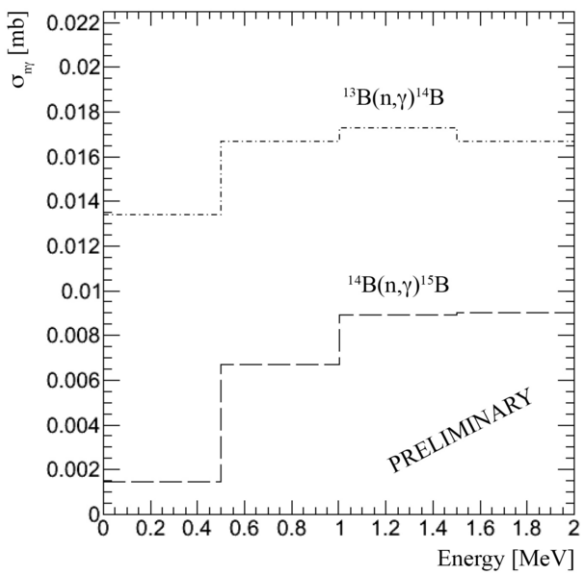


FIG. 5. The  $^{13,14}\text{B}(n, \gamma)$  cross-sections derived from the corresponding Coulomb breakup of  $^{14}\text{B}$  and  $^{15}\text{B}$ .

an integration limit of 10 MeV in excitation energy for the Coulomb breakup of  $^{14}\text{B}$  and  $^{15}\text{B}$  are 308 mb and 81 mb, respectively. By taking the virtual photon distribution into account and applying the principle of detailed balance the corresponding neutron capture cross-sections (Fig. 5) are derived from the measured Coulomb dissociation cross-sections. The uncertainties are still under analysis, but are estimated to be about 10%. The one-neutron halo nucleus  $^{11}\text{Be}$ , which was included in the same beam setting, was used as a test-case since it has been already studied in previous experiments [7], [8]. The analysis of the  $^{11}\text{Be} \rightarrow ^{10}\text{B}+n$  reaction results in a preliminary integral cross-section up to an integration limit of 5.6 MeV in excitation energy of  $\sigma_{CD} = 471$  mb at about 490 AMeV in comparison to  $\sigma_{CD} = 477(32)$  mb at about 520 AMeV measured by Palit *et al.* [7]. The dipole strength  $B(E1)$  was determined to be  $0.87 \text{ e}^2\text{fm}^2$ , while Palit derived  $B(E1) = 0.83(6) \text{ e}^2\text{fm}^2$  and Fukuda *et al.*  $B(E1) = 1.05(6) \text{ e}^2\text{fm}^2$  [8]. The preliminary results obtained within the presented experiment are in good agreement with previous experimental studies.

#### IV. SUMMARY AND OUTLOOK

The Coulomb breakup of  $^{14,15}\text{B}$  has been successfully performed at the LAND/R<sup>3</sup>B-setup at GSI and the analysis is still in progress. Preliminary results for the differential Coulomb dissociation cross-sections and the corresponding neutron capture cross-sections were derived. In the same manner the analysis of  $^{11}\text{Be}$  was performed as a test-case and the results are in good agreement with previous experiments. The stellar reaction rates will be derived from the experimentally obtained neutron capture cross-sections and model calculations for the *r*-process nucleosynthesis will be performed to study the impact on the final *r*-process abundances to these light neutron-rich isotopes.

*Acknowledgements:* This project was supported by the Helmholtz International Center for FAIR, the Helmholtz Young Investigator Group VH-NG-327 and the Helmholtz Alliance Program of the Helmholtz Association, Contract No. HA216/EMMI.

[1] J. Witt *et al.*, ASTRON. ASTROPHYS. **286**, 841 and 857 (1994).  
 [2] S.E. Woosley *et al.*, ASTROPHYS. J. **433**, 229 (1994).  
 [3] J. Truran *et al.*, PUB. ASTR. SOC. PAC. **114**, 1293 (2002).

[4] M. Terasawa *et al.*, ASTROPH. J. **562**, 470 (2001).  
 [5] T. Sasaqui *et al.*, ASTROPH. J. **643**, 1173 (2005).  
 [6] J. Cub *et al.*, NUCL. INST. METHODS **A 402**, 67 (1998).  
 [7] R. Palit *et al.*, PHYS. REV. C **48**, 034318 (2003).  
 [8] N. Fukuda *et al.*, PHYS. REV. C **70**, 054606 (2004).